MOLECULAR AND CELLULAR BIOLOGY, Nov. 2007, p. 7462–7474 Vol. 27, No. 21
0270-7306/07/$08.00+0 doi:10.1128/MCB.01120-07

Acetylation-Induced Transcription Is Required for Active DNA Demethylation in Methylation-Silenced Genes[▽]

Ana C. D'Alessio, Ian C. G. Weaver, and Moshe Szyf*

Department of Pharmacology and Therapeutics, McGill University, Montreal, Quebec H3G 1Y6, Canada

Received 23 June 2007/Returned for modification 5 July 2007/Accepted 9 August 2007

A hallmark of vertebrate genes is that actively transcribed genes are hypomethylated in critical regulatory sequences. However, the mechanisms that link gene transcription and DNA hypomethylation are unclear. Using a trichostatin A (TSA)-induced replication-independent demethylation assay with HEK 293 cells, we show that RNA transcription is required for DNA demethylation. Histone acetylation precedes but is not sufficient to trigger DNA demethylation. Following histone acetylation, RNA polymerase II (RNAP II) interacts with the methylated promoter. Inhibition of RNAP II transcription with actinomycin D, α-amanitin, or CDK7-specific small interfering RNA inhibits DNA demethylation. H3 trimethyl lysine 4 methylation, a marker of actively transcribed genes, was associated with the cytomegalovirus promoter only after demethylation. TSA-induced demethylation of the endogenous cancer testis gene *GAGE* follows a similar sequence of events and is dependent on RNA transcription as well. These data suggest that DNA demethylation follows rather than precedes early transcription and point towards a novel function for DNA demethylation as a memory of actively transcribed genes.

The epigenome programs gene expression profiles of vertebrate cells. The epigenome is composed of chromatin structure and DNA methylation. The basic unit of chromatin, the nucleosome, is composed of histones, which undergo an assortment of covalent modifications in their N-terminal tails, including phosphorylation, acetylation, methylation, and ubiquitination (57, 66). These modifications affect the structural dynamics of the nucleosome by forming a "histone code" that regulates chromatin function through the recruitment of specific interacting proteins that recognize a single or conformational set of modifications.

The other component of the epigenome, DNA methylation, is a covalent modification of cytosines residing at CpG dinucleotides in vertebrate genomes (47). Actively transcribed chromatin regions are distinguished by hypomethylated DNA (46, 48), whereas many inactive genes, such as parentally imprinted genes and tumor suppressor genes in cancer, are hypermethylated in critical regions and associate with hypoacetylated lysine 9-methylated histone tails (21). A recent high-resolution analysis of DNA methylation patterns and histone H3 and H4 acetylation patterns in the HOXA cluster region revealed no acetylated histones in the hypermethylated regions, demonstrating a reciprocal relationship between DNA methylation and histone H3 and H4 acetylation (23).

Although DNA methylation is associated with silencing of several genes, such as tumor suppressor genes in cancer (2), the relationship between DNA methylation and gene transcription is complex. A recent comprehensive analysis of the human methylome revealed that CG-rich islands are almost uniformly unmethylated, irrespective of their state of expression, while CG-poor genes are generally methylated (63). The fact that CG islands are unmethylated, even in the absence of transcription, seems to suggest that a mechanism other than transcription "per se" is responsible for the hypomethylated state.

Interestingly, the same authors identified an inverse correlation between methylation and expression in promoters with intermediate CG density; this suggests that a mechanism exists to coordinate transcription and DNA demethylation, at least in this fraction of the promoters in the human genome. These promoters were for germ line-specific genes, which are methylated in somatic cells, hypomethylated in the testis (63), and induced by DNA-demethylating agents (55). We therefore focused this study on the cytomegalovirus (CMV) promoter as a probe to study replication-independent demethylation of an intermediate CG promoter and demethylation of *GAGE*, a testis-specific gene. The remaining issue is determining the mechanisms which lead to demethylation of genes and to maintenance of their unmethylated state.

Several lines of evidence suggest that the "histone code" regulates the level of DNA methylation. This epigenetic cross talk has been studied extensively for chromatin silencing. Firstly, DIM-5 from the fungus *Neurospora crassa* and kryptonite from *Arabidopsis thaliana*, two histone methyltransferases for lysine 9, were shown to be important for normal DNA methylation (24, 25, 59). Secondly, targeted deletion of Lsh, a member of the SNF2/helicase family involved in chromatin remodeling, produces a substantial loss of CpG methylation throughout the genome (65). In addition, EZH2, a member of the multiprotein Polycomb complex PRC2, which methylates histone H3 at K27, is important for the establishment of new methylation patterns (61).

Work from our laboratory demonstrated that there is also an epigenetic activation cross talk (7, 13). We showed that inhibition of histone deacetylases (HDACs) by trichostatin A (TSA) triggers active DNA demethylation of an in vitro methylated nonreplicating plasmid introduced into HEK 293 cells.

* Corresponding author. Mailing address: Department of Pharmacology and Therapeutics, McGill University, 3655 Promenade Sir William Osler, Montreal, Quebec H3G 1Y6, Canada. Phone: (514) 398-7107. Fax: (514) 487-1834. E-mail: moshe.szyf@mcgill.ca.

▽ Published ahead of print on 20 August 2007.

In addition, blockage of histone acetylation by the expression of inhibitors of histone acetylation proteins inhibited demethylation by TSA, supporting the hypothesis that histone acetylation rather than side effects of the HDAC inhibitor triggered demethylation (6). A recent comprehensive analysis of human promoters revealed a correlation between lack of methylation and H3K4 dimethylation, leading the authors to suggest that chromatin modification might protect CG-rich islands from methylation (63).

Here we test the hypothesis that chromatin activation "per se" leads to DNA demethylation. To gain insights into the mechanisms linking chromatin modification, gene activation, and DNA demethylation, we delineated their temporal relationship following histone hyperacetylation induced by TSA. Our findings suggest that DNA demethylation is a stepwise, highly coordinated process that involves histone acetylation and, importantly, RNA polymerase II (RNAP II) transcription. To our surprise, our findings indicate that DNA demethylation follows rather than precedes early transcription. Following DNA demethylation, histones associated with the CMV-green fluorescent protein (CMV-GFP) plasmid are trimethylated on lysine 4 (H3K4me3). H3K4me3, a memory of actively transcribed genes (38, 50), is selectively associated with unmethylated copies of the CMV promoter. We show that RNA transcription by RNAP II is required for DNA demethylation, suggesting that the epigenetic reprogramming of genes requires an initial state of transcription. Our results are consistent with the hypothesis that DNA demethylation plays a role in the stable memory of RNAP II-mediated transcription, since early transcription of a methylated promoter results in its demethylation, which enhances and stabilizes its active state.

MATERIALS AND METHODS

Plasmids. pEGFP-C2 (pCMV-GFP) was purchased from Clontech (GenBank accession number U55763). A CDK7 short hairpin RNA-expressing plasmid was purchased from Upstate Biotechnology. The negative control, which does not target any sequence contained in the human genome, was provided by a pSilencer 2.1-U6 neo kit from Ambion.

In vitro methylation of plasmid DNA. pCMV-GFP was methylated in vitro as described previously (7).

Cell culture and transient transfections. HEK 293 cells were plated at a density of 0.5×10^6 in a 10-cm plate and transiently transfected with 500 ng of methylated pCMV-GFP, using the calcium phosphate precipitation method. Three hundred nanomolar TSA was added at 24 h posttransfection. Cells were harvested at different times after initiation of TSA treatment. Each experiment was performed in triplicate.

Bisulfite mapping. Bisulfite mapping was performed as described previously, with minor modifications (9). Five micrograms of sodium bisulfite-treated DNA sample was subjected to PCR amplification using a first set of primers, and the PCR products were used as templates for a subsequent PCR utilizing nested primers. The primers used for the CMV promoter (pCMV-GFP) (Clontech) were CMV-outside-sense (5′-GTT TAG TAT ATG ATT TTA TGG G-3′), CMV-outside-antisense (5′-CCA AAA TAA ACA CCA CCC C-3′), CMV-nested-sense (5′-ATT TTT TTA TTT GGT AGT ATA TTTA-3′), and CMV-nested-antisense (5′-CCC TTA CTC ACC ATA ATA AC-3′); the primers for the GFP coding region were GFP-outside-sense (5′-GTT ATT ATG GTG AGT AAG GG-3′), GFP-outside-antisense (5′-TAT AAC TAT TAT AAT TAT ACT CCA-3′), GFP-nested-sense (5′-GGG GTG GTG TTT ATT TTG G-3′), and GFP-nested-antisense (5′-CTT ATA CCC CAA AAT ATT ACC-3′); the primers for the simian virus 40 (SV40) polyadenylation site were PA-outside-sense (5′-TTA TTG TAT TTT AGT TGT GGT-3′), PA-outside-antisense (5′-AAA ACT CCC TTT AAA ATT CC-3′), PA-nested-sense (5′-TTG TTT AAA TTT ATT AAT GTA TTT AA-3′), and PA-nested-antisense (5′-CAA AAA ACT TAA TTA AAA TAA TTC-3′); the primers for the *GAGE* promoter were GAGEprom-outside-sense (5′-GTT TAT ATT GAA TAA TTT TTT TTT G-3′), GAGEprom-outside-antisense (5′-ATC TCA ATA AAA AAA AAA AAA TCC-3′), GAGEprom-nested-sense (5′-GAA TAG GTT GTT ATT TTT GTT T-3′), and GAGEprom-nested-antisense (5′-TAC CTC ACA ACT CCC TAA C-3′); and the primers for the first *GAGE* exon were GAGEcoding-outside-sense (5′-TTA GGG AGT TGT GAG GTA G-3′), GAGEcoding-outside-antisense (5′-CCC CAC TCA CAA CAA ATT TA-3′), GAGEcoding-nested-sense (5′-ATT TAT TTG GTA GGT GTG TAG-3′), and GAGEcoding-nested-antisense (5′-CCT TAC AAT ACT TCT CAC TC-3′). The PCR products of the second reaction were then subcloned using an Invitrogen TA cloning kit following the manufacturer's protocol. The clones were sequenced using a T7 sequencing kit as recommended by the manufacturer (procedure C; Amersham Pharmacia Biotech).

ChIP assays. Chromatin immunoprecipitation (ChIP) assays (12) were done using a ChIP assay kit protocol (Upstate Biotechnology). HEK 293 cells were transfected with 500 ng of methylated pCMV-GFP, using the calcium phosphate precipitation method as described below. Three hundred nanomolar TSA was added at 24 h posttransfection. Formaldehyde was added to the culture medium at a final concentration of 1% at different times after initiation of TSA treatment, and the cells were incubated for 10 min at 37°C. Chromatin was immunoprecipitated using the following antibodies: anti-acetylated histone H3 (Upstate Biotechnology), anti-polymerase II (anti-Pol II; Santa Cruz), anti-trimethylated K4 H3 (Abcam), and normal rabbit immunoglobulin G (IgG; Santa Cruz). One-tenth of the lysate was kept to quantify the amount of DNA present in the different samples before immunoprecipitation. PCRs on DNAs purified from nonimmunoprecipitated and immunoprecipitated samples were quantified in triplicate by real-time PCR, using PowerSYBR green PCR master mix (Applied Biosystems). Input samples were diluted 1/40, whereas antibody and IgG samples were diluted 1/10. The following primers were used: CMV sense, 5′-CAC CAA AAT CAA CGG GAC TTT C-3′; CMV antisense, 5′-TAC ACG CCT ACC GCC CAT T-3′; GFP sense, 5′-GAC GGA AAC GGC CAC AAG TTC-3′; GFP antisense, 5′-TTG CCG GTG GTG CAG AT-3′; GAGE prom sense, 5′-TAC TTG AGT CCC AGA GGC ATA GG-3′; GAGE prom antisense, 5′-CCT CCA TGC CCA TCC TCA T-3′; GAGE exon1 sense, 5′-TTT TTC CTC TAC TGA GAT TCA TCT GGT A-3′; GAGE exon1 antisense, 5′-CTC CAC CCT CAC TCA CAC TTC A-3′; GLOBIN Delta sense, 5′-CTG TCT GTG AAT GAA AAG AAG GAA AT-3′; GLOBIN Delta antisense, 5′-CTA CGT TCA TTG CCA GAT CCA A-3′; LACZ sense, 5′-CCC ATC TAC ACC AAC GTA ACC TAT C-3′; and LACZ antisense, 5′-GAG TAA CAA CCC GTC GGA TTC T-3′. Amplifications were performed with an ABI 7900 HT sequence detection system, using the following protocol: 50°C for 2 min, 95°C for 10 min, and 40 cycles of 95°C for 15 s and 60°C for 1 min.

Northern and Southern blot analysis. For Northern blot analysis, approximately 2 μg of RNA was electrophoresed in a 1.2% denaturing agarose gel and then transferred with 10× SSC (1× SSC is 0.15 M NaCl plus 0.015 M sodium citrate) to a Hidrobond-N+ membrane (Amersham Pharmacia Biotech). Southern blot analysis was performed as described previously (7). The levels of expression of the different mRNAs in the Northern blots were quantified by densitometric scanning of the relevant autoradiograms. Each experiment was normalized for the amount of total RNA by hybridization with a ^{32}P-labeled 18S rRNA oligonucleotide probe.

Western blot analyses. Twenty-five micrograms of proteins was loaded into a 10% sodium dodecyl sulfate-polyacrylamide gel. After the proteins were transferred to a nitrocellulose membrane and blocked with 5% skim milk, CDK7 protein was detected using rabbit polyclonal IgG (Abcam) at a 1:500 dilution, followed by peroxidase-conjugated anti-rabbit IgG (Sigma) at 1:5,000. Actin Western blots were performed using a 1:5,000 dilution of actin monoclonal antibody (Sigma) followed by the mouse secondary antibody at 1:20,000 (Jackson ImmunoResearch). An enhanced chemiluminescence kit (Amersham Biosciences) was used for all Western blots.

Microarray analysis. Human embryonic kidney HEK 293 cells (ATCC CRL 1573) were plated at a density of 0.5×10^6 cells in a 10-cm plate. Twenty-four hours later, 300 nM TSA was added for 72 h. Total RNA was extracted with RNeasy (QIAGEN). Microarray analysis was performed as previously described (18). Briefly, 20 μg of RNA was used for cDNA synthesis, followed by in vitro transcription with a T7 promoter primer containing a poly(T) tail. The resulting product was hybridized to a HuGeneFL DNA microarray containing oligonucleotides specific for 20,000 human transcripts and then processed with a GeneChip system (Affymetrix). Data analysis, average difference, and expression for each feature on the chip were computed using the Affymetrix GeneChip analysis suite, version 3.3, with default parameters. Each experiment was performed in duplicate. The Montreal Genome Centre performed the gene expression analysis.

Reverse transcription-PCR (RT-PCR). Total RNA was extracted using the standard guanidinium isothiocyanate method. cDNA was synthesized in a 20-μl reaction volume containing 5 μg of total RNA, 40 units of Moloney murine leukemia virus reverse transcriptase (MBI), 5 μM of random primers (Roche Molecular Biochemicals), a 1 mM concentration of each of the four deoxynucleoside triphosphates, and 40 units of RNase inhibitor (Roche Molecular Biochemicals). mRNA was denatured for 5 min at 70°C, the random primers were annealed for 10 min at 25°C, and mRNA was reverse transcribed for 1 h at 37°C. The reverse transcriptase was heat inactivated at 70°C, and the products were stored at −20°C until use. PCR was performed in a 30-μl reaction mixture containing 2 μl of synthesized cDNA product, 3 μl of 10× PCR buffer, 2 mM $MgCl_2$, a 0.2 mM concentration of each deoxynucleoside triphosphate, 1 unit *Taq* polymerase (all from MBI), and 0.5 μM of each primer.

Quantitative RT-PCR. Quantitative PCRs were performed as described previously, using PowerSYBR green PCR master mix (Applied Biosystems) and the following primers: GAGE sense, 5′-GCT GCT CAG AAG GGA GAG GAT-3′; GAGE antisense, 5′-CTG TTC CTG GCT ATG AGC TTC A-3′; GFP sense, 5′-GAC GGA AAC GGC CAC AAG TTC-3′; and GFP antisense, 5′-TTG CCG GTG GTG CAG AT-3′. For glyceraldehyde-3-phosphate dehydrogenase (GAPDH) gene amplification, a human GAPD endogenous control (FAM/MGB probe; non-primer-limited TaqMan predeveloped assay reagents [Applied Biosystems]) was used with TaqMan Universal PCR master mix (Applied Biosystems). For *CGA*, *SPANAX1*, and *ARC* amplifications, a universal probe library set from Roche was used (for *CGA*, probe 61 was used; for *SPANAX1*, probe 68 was used; and for *ARC*, probe 21 was used) with FastStart TaqMan probe master mix from Roche. All amplifications were performed with an ABI 7900 HT sequence detection system, using the following protocol: 50°C for 2 min, 95°C for 10 min, and 40 cycles of 95°C for 15 s and 60°C for 1 min.

RESULTS

Time course of demethylation of ectopically methylated CMV promoter following TSA treatment. DNA demethylation in a replicating cell can be either an active or a passive replication-dependent process. To distinguish between these two possibilities, we took advantage of a previously developed active demethylation assay using living HEK 293 cells (7). In this system, pharmacological induction of histone acetylation by HDAC inhibition with TSA triggers active DNA demethylation of ectopically methylated pCMV-GFP. We have previously shown, using the DpnI restriction enzyme, which digests only DNA that maintains its bacterial methylation (GmATC) pattern, that pCMV-GFP did not replicate in HEK 293 cells during the course of the experiment (7). This was also repeated here to verify that the demethylation events studied were indeed active (data not shown). In this study, we used ChIP assays with pertinent histone modification antibodies and bisulfite mapping to study the temporal and causal relationship between chromatin and active DNA demethylation.

We first measured the time course of demethylation of the CMV promoter (Fig. 1A; also see Fig. 3, left panel). Bisulfite mapping of transfectants treated with 300 nM TSA for different times showed that DNA demethylation increases over time and is a slow process, starting at 18 h and being completed only after 48 h of TSA treatment.

Histone acetylation is not sufficient to trigger DNA demethylation of the ectopically methylated CMV promoter. To test the hypothesis that histone acetylation per se is the only change required for DNA demethylation, we analyzed the time course of histone H3 acetylation at the CMV promoter following TSA treatment, using ChIP analysis. We found that histone acetylation (Fig. 1B) precedes DNA demethylation (Fig. 1A; also see Fig. 3). These data suggest that there is a lag between histone acetylation and demethylation. To directly assess whether histone acetylation triggers immediate DNA demethylation, we

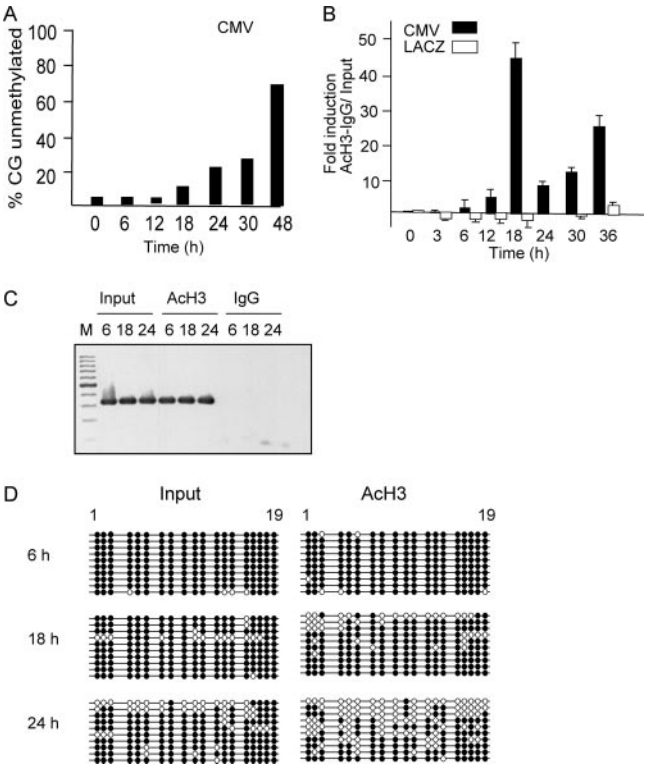

FIG. 1. Histone acetylation precedes DNA demethylation. In vitro-methylated pCMV-GFP plasmid was transfected into HEK 293 cells and treated with TSA at 24 h posttransfection. Cells were harvested at different time points of TSA treatment. (A) Time course of active DNA demethylation. DNA was subjected to bisulfite methylation mapping analysis. The CMV region was amplified, subcloned, and sequenced as described in Materials and Methods. Each bar represents the average for 10 different clones at each site. (B) ChIP assay using an antibody against either H3K9Ac or control IgG. Samples were spiked with LacZ prior to immunoprecipitation to rule out nonspecific DNA precipitation with the antibody. The CMV and negative control LacZ sequences were amplified from purified DNA by quantitative PCR. (C) Representative bisulfite PCR amplification from input DNA and DNAs purified from immunoprecipitated acetyl histone H3 and IgG samples. (D) The DNAs used for panel C were subjected to bisulfite mapping analysis. Each line represents one clone. Filled circles, methylated CG dinucleotides within the CMV promoter; open circles, demethylated CG dinucleotides.

measured the state of methylation of pCMV-GFP DNA associated with acetylated histones early after TSA induction by using a combination of ChIP and bisulfite mapping. Input, anti-acetyl-H3 (H3K9Ac), and IgG ChIP DNAs prepared from transfectants treated with TSA for different times were subjected to bisulfite PCR (Fig. 1C) and mapping (Fig. 1D). Sodium bisulfite DNA amplification was observed in the input and immunoprecipitated H3K9Ac samples but not in the immunoprecipitated IgG or water control sample (Fig. 1C), indicating that the bisulfite-sequenced material represents DNA associated with H3K9Ac histones. If histone acetylation were the only rate-limiting step for demethylation, we would expect that as soon as CMV-GFP is associated with acetylated histone H3, it would be demethylated straight away, even at the early 6-h time point. However, we observed that the molecules associated with H3K9Ac were methylated at 6 h and only became

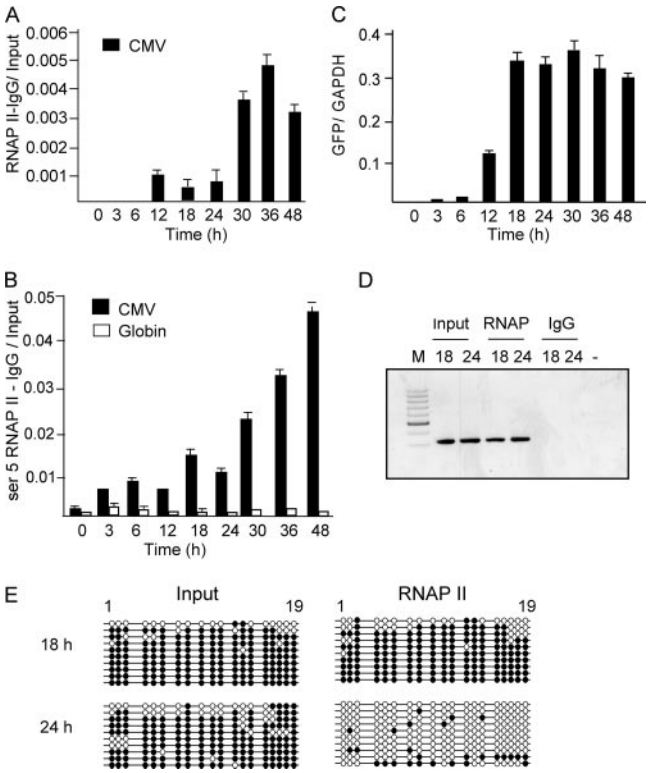

FIG. 2. RNAP II transcribes and binds the methylated CMV promoter. In vitro-methylated pCMV-GFP was transfected into HEK 293 cells, and at 24 h posttransfection, cells were treated with TSA. Cells were harvested at different time periods of TSA treatment. (A and B) Cells were subjected to ChIP assay using an anti-RNAP II antibody (A) or an antibody against the serine 5-phosphorylated form of the CTD of RNAP II (B) or were processed with IgG. The CMV sequence was amplified from purified DNA by quantitative PCR. As a negative control, a region 5 kb upstream of the globin delta gene was amplified by quantitative PCR. No amplification of the globin delta gene was observed in the RNAP II ChIP samples. (C) Kinetics of GFP expression after TSA treatment. Quantitative real-time RT-PCR of the GFP and GAPDH genes was performed. The ratios of the GFP to GAPDH signals were plotted. No signal was observed in the no-RT control. (D) Representative bisulfite PCR amplification from input DNA and DNAs purified from immunoprecipitated RNAP II and IgG samples. (E) The DNAs used for panel D were subjected to bisulfite mapping analysis. Each line represents one clone. Filled circles, methylated CG dinucleotides within the CMV promoter; open circles, demethylated CG dinucleotides.

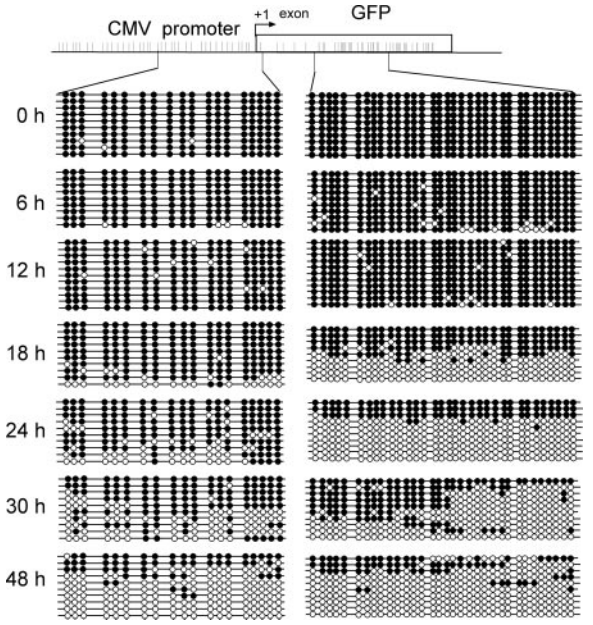

FIG. 3. Time course of active DNA demethylation after TSA treatment. In vitro-methylated pCMV-GFP was transfected into HEK 293 cells, and at 24 h posttransfection, cells were treated with TSA. Cells were harvested at different time periods of TSA treatment. DNAs prepared from transfectants treated with TSA for different periods were subjected to bisulfite methylation mapping analysis. The *CMV* and *GFP* regions were amplified, subcloned, and sequenced as described in Materials and Methods. Each line represents one clone. Filled circles, methylated CG dinucleotides within the CMV promoter; open circles, demethylated CG dinucleotides.

demethylated 24 h after the addition of TSA (Fig. 1D), indicating that other events in addition to H3 acetylation might be required for DNA demethylation following TSA treatment.

Time course of DNA demethylation and transcription. If DNA demethylation plays a causal role in gene expression, then it is expected that demethylation would precede transcription. To address this, we studied the time course of GFP transcription and CMV demethylation after TSA treatment (Fig. 2C and 3). RNA transcription started between 3 h and 12 h after TSA treatment (Fig. 2C); however, no DNA demethylation was observed at these time points (Fig. 1A and 3). DNA demethylation was first detected at the 18-h time point (Fig. 1A and 3). This is consistent with the notion that transcription preceded DNA demethylation.

A ChIP experiment with an anti-RNAP II antibody revealed that occupancy of the CMV promoter with RNAP II following TSA treatment is detectable 12 h following TSA treatment (Fig. 2A). Transcription of genes by RNAP II is a complex process (11, 32, 36, 40, 41) and, as such, requires a highly coordinated and multistep process utilizing a large number of basal and transactivating factors. Furthermore, there exists a dynamic association of mRNA processing factors with differently modified forms of the polymerase throughout the transcription cycle (31). More specifically, the phosphorylation of the C-terminal domain (CTD) in RNAP II at serine 5 has been associated with transcription initiation. Using a ChIP experiment against this phosphorylated form of RNAP II, we were able to control for initiation of the transcription process. An excellent correlation was observed between GFP expression (Fig. 2C) and serine 5 phosphorylation of the CTD of RNAP II (Fig. 2B). The small discrepancy between the initiation of binding of RNAP II and its serine 5-phosphorylated form could be due to differences in antibody sensitivity and dynamic range.

RNAP II binds the methylated CMV promoter during RNA transcription. We resorted again to a combination of ChIP and bisulfite mapping to determine whether demethylation is a prerequisite for binding of RNAP II. If demethylation were a precondition for RNAP II interaction, then CMV promoters bound to RNAP II would be demethylated even at the earliest time point when RNAP II binding to CMV is detected. However, if demethylation follows RNAP II interaction with methylated DNA, RNAP II would initially bind to methylated CMV

promoters. Sodium bisulfite DNA amplification was observed in the input and immunoprecipitated RNAP II samples but not in the immunoprecipitated IgG or water control sample (Fig. 2D). DNAs amplified from anti-RNAP II ChIP and input samples were subjected to bisulfite mapping. Interestingly, our data show that CMV promoter sequences bound to RNAP II were methylated at 18 h (Fig. 2E), implying that RNAP II initially binds to methylated CMV promoters. At 24 h, RNAP II-bound CMV promoters were enriched with unmethylated copies in comparison with the input DNA, suggesting that CMV promoters bound to RNAP II are targeted for demethylation. Promoters that are not loaded with RNAP II and are not actively transcribed remain methylated.

Since RNAP II binds a methylated CMV promoter, the question raised is whether demethylation starts at the promoter or downstream of the transcription initiation site. A time course analysis of demethylation of the CMV promoter and the GFP coding sequence showed that demethylation of the CMV promoter lags behind demethylation of the *GFP* sequence (Fig. 3). This is consistent with the hypothesis that demethylation initiates along the path of transcription of RNAP II and then spreads to the promoter sequence.

RNA transcription is required for DNA demethylation. To test the hypothesis that transcription elongation is required for demethylation, we used two well-characterized pharmacological inhibitors of RNAP II transcription activity, namely, α-amanitin and actinomycin D. Actinomycin D is a DNA-intercalating agent which is believed to stall the progression of RNAP II but does not inhibit transcription initiation (29). α-Amanitin interacts with the "funnel," "cleft," and "bridge α-helix" regions of the Rbp1 subunit of RNAP II and is believed to inhibit elongation at each translocation step of the RNA-DNA hybrid (5, 19). Methylation-sensitive Southern blot analysis of the GFP coding region showed that actinomycin D inhibits DNA demethylation (Fig. 4D). On the other hand, the protein synthesis inhibitor cycloheximide did not inhibit DNA demethylation, suggesting that the effect that inhibition of transcription had on demethylation was not caused by a change in the cellular levels of a "high-turnover" demethylation factor. In addition, pretreatment of the cell with cycloheximide prior to TSA treatment had no effect on DNA demethylation (Fig. 4E), further excluding the possibility that our actinomycin treatment inhibited DNA demethylation through blocking the synthesis of a labile high-turnover protein required for DNA methylation.

Our data suggest that RNA transcription, but not protein synthesis, is required for demethylation. Figure 4B shows that actinomycin D, but not cycloheximide, inhibited GFP mRNA as expected; however, cycloheximide inhibited GFP protein synthesis to an even larger extent than the inhibition by actinomycin D (Fig. 4C). Bisulfite mapping of the promoter and transcribed *GFP* regions showed that actinomycin D inhibited DNA demethylation both at the *GFP* transcribed sequence and at the promoter (Fig. 4F). If progression of RNAP II were indeed required for DNA demethylation, inhibition of transcript elongation by RNAP II with α-amanitin should have the same effect as actinomycin D. As expected, α-amanitin inhibited DNA demethylation at the *GFP* transcribed region (Fig. 4F). To further prove that DNA demethylation requires progression of RNAP II, we mapped the state of methylation of CG sites residing downstream of the SV40 polyadenylation site at the 3′ end of the GFP coding sequence. If DNA demethylation is linked to transcription, DNA demethylation would stop at the point where transcription terminated. As expected, CGs downstream of the polyadenylation signal remained methylated at 48 h of TSA treatment, whereas CGs upstream of the point of transcription termination were demethylated (Fig. 4G). Thus, transcription is required for DNA demethylation.

siRNA depletion of CDK7 inhibits DNA demethylation. In order to test the relationship between transcription and DNA demethylation, we performed small interfering RNA (siRNA) knockdown of CDK7, a protein kinase which is found at the transcription initiation complex and phosphorylates the CTD of RNAP II (53, 54), regulating the step between transcription initiation and elongation. A Western blot analysis with anti-CDK7 shows CDK7 knockdown by the siRNA treatment (Fig. 5A). Supporting the hypothesis that transcription is required for demethylation, CDK7 knockdown resulted in decreased GFP expression (Fig. 5B) as well as a reduction in the extent of DNA demethylation of the *GFP* transcribed sequence and the CMV promoter (Fig. 5C). In summary, different manipulations that inhibit the progression of RNAP II by distinct mechanisms inhibit DNA demethylation, suggesting a causal relationship between passage of RNAP II and DNA demethylation. CDK7 knockdown had a smaller effect on DNA demethylation than did inhibition of transcription with small molecules. This probably reflects a more effective blockage of transcription by inhibitors of RNAP II progression than that by CDK7 knockdown.

The GFP coding region associates with H3K4me3 after the CMV promoter is demethylated. H3K4me3 is a hallmark of genes programmed to be active (22, 38, 49, 50). SET1, the histone methyltransferase for lysine 4, associates with the newly initiated RNAP II following phosphorylation of serine 5 of the CTD (38).

If DNA demethylation indeed sets the stage for stable programming of gene activity, we predict that H3K4me3 will occur after DNA demethylation and that CMV promoters associated with H3K4me3 will be enriched in unmethylated DNA. To test this hypothesis, we followed the time course of H3K4me3 association with the GFP gene following TSA treatment, using ChIP analysis. H3K4me3 (Fig. 6A) occurred after DNA demethylation (Fig. 1A). The human homolog of yeast SET1 is one of the enzymes responsible for H3K4 methylation. Analysis of the time course of SET1 occupancy of the CMV promoter revealed a correlation between SET1 occupancy and H3K4me3 at the *GFP* exon (Fig. 6B).

Furthermore, we determined the state of methylation of CMV promoter DNA associated with H3K4me3 at the earliest time point by using a combination of ChIP and bisulfite mapping analysis. Sodium bisulfite DNA amplification was observed in the input and immunoprecipitated H3K4me3 samples but not in the immunoprecipitated IgG or water control sample (Fig. 6C). H3K4me3-bound CMV-GFP contained promoter DNA that was significantly more demethylated than the input DNA (Fig. 6D and E). This interesting pattern of hypomethylation suggests a selection for unmethylated DNA associated with H3K4me3 histones.

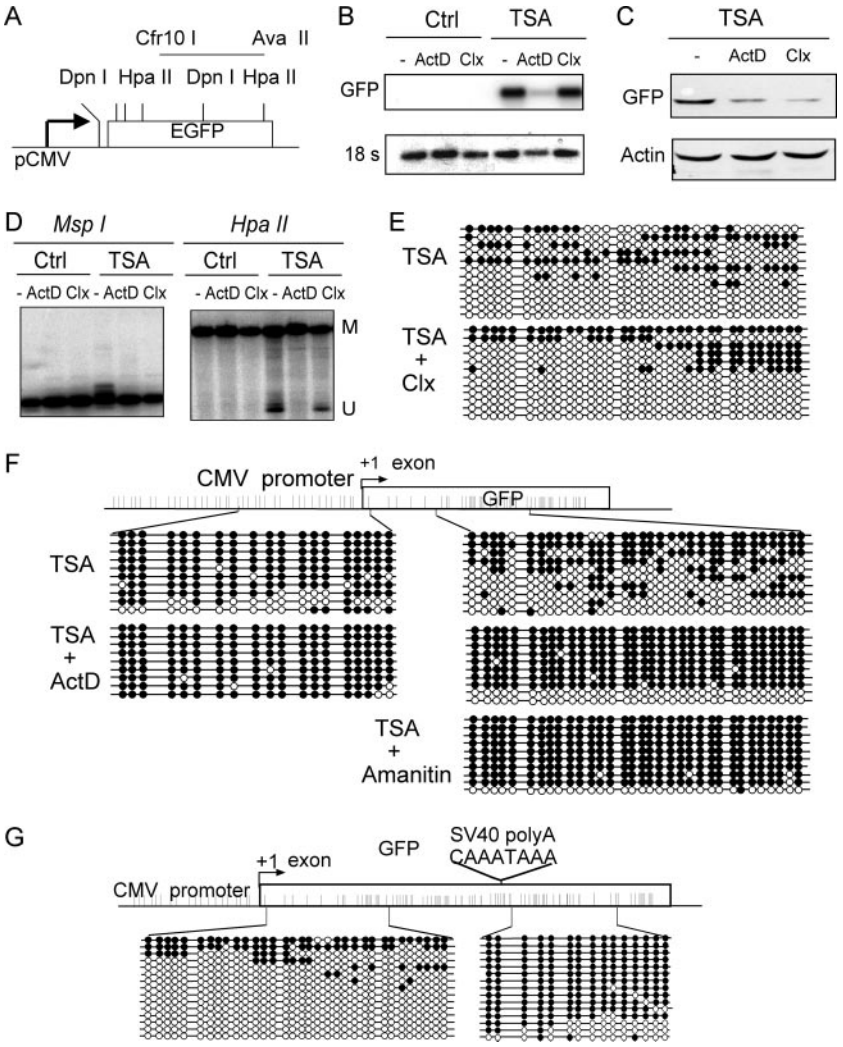

FIG. 4. Transcription is required for DNA demethylation. (A) Physical map of the *GFP* region analyzed by Southern blotting. (B to D and F) In vitro-methylated pCMV-GFP was transfected into HEK 293 cells, and at 24 h posttransfection, cells were treated with TSA for 30 h or left untreated as a control. At 18 h of TSA treatment, cells were treated with actinomycin D (ActD; 1 μg/ml) or cycloheximide (Clx; 4 μM) or left untreated as a control for 12 h. (B) mRNA levels for *GFP* were determined by Northern blot analysis with probes for *GFP* and 18S rRNA. (C) Western blot analysis of GFP and actin. (D) DNA demethylation analysis by methylation-sensitive Southern blotting as described in Materials and Methods. U, unmethylated DNA; M, methylated DNA. (E) In vitro-methylated pCMV-GFP was transfected into HEK 293 cells. At 24 h posttransfection, cells were pretreated with cycloheximide (4 μM) for 28 h or left without pretreatment as a control. Cells were treated with TSA for 24 h. Bisulfite mapping analysis of the *GFP* region is shown. (F) Bisulfite mapping analysis. Actinomycin D and α-amanitin were introduced at final concentrations of 1 μg/ml and 10 μg/ml, respectively. (G) HEK 293 cells were treated with TSA for 48 h. DNAs were subjected to bisulfite methylation mapping analysis. The *GFP* gene and the region downstream of the SV40 polyadenylation signal were amplified, subcloned, and sequenced. Filled circles, methylated CG dinucleotides; open circles, demethylated CG dinucleotides.

Endogenous genes are demethylated in response to TSA treatment. The advantage of the transiently transfected CMV-GFP system is that it enables an analysis of replication-independent active demethylation in dissociation from passive, replication-dependent demethylation in living cells. Although the plasmid DNA associates with histones, which undergo a regulated series of modifications, it is not fully chromatinized. This raised the issue of whether TSA would induce demethylation of an endogenous gene as well.

We first identified genes induced by TSA in our HEK 293 model system by using expression microarray analysis. Fewer than 1% of the genes were found to be induced and 0.2% were suppressed by TSA (Fig. 7A and B), suggesting significant selectivity of TSA in our system. Table 1 shows the identities of the top 29 genes induced by TSA. The induction by TSA of a sample of genes in the gene array was validated by RT-PCR (Fig. 7D). Methylation of DNA acts as an on-off switch, and therefore we focused on genes which showed an off-on response to TSA as candidates to be regulated by DNA methylation. The cancer-testis antigen family (CT antigens) (Fig. 7C) fits precisely into this description for our array. The genes in this family are heavily methylated in normal tissues but are demethylated specifically in the testis and, interestingly, are also demethylated in many highly invasive cancers whose DNAs are globally hypomethylated. CT antigens were previously shown to be induced by the DNA methylation inhibitor

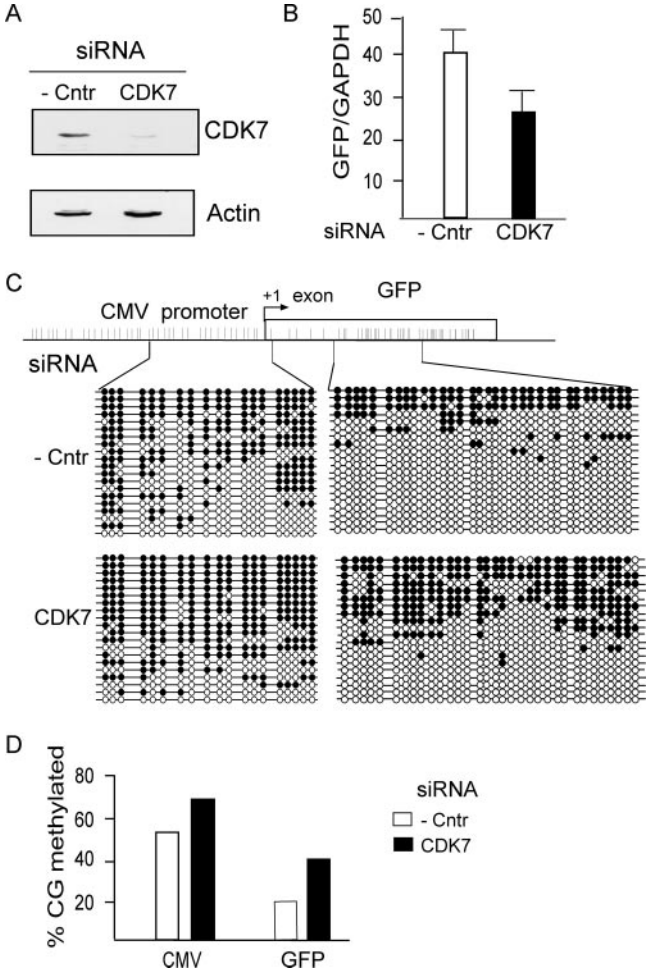

FIG. 5. siRNA knockdown of CDK7 decreases the extent of TSA-induced DNA demethylation. In vitro-methylated pCMV-GFP was cotransfected into HEK 293 cells with either a CDK7 or negative control siRNA expression plasmid, as described in Materials and Methods. The cells were treated at 48 h posttransfection with a final concentration of 300 nM TSA for an additional 48 h. (A) Western blot analysis of negative control and CDK7 siRNAs, using anti-CDK7 and anti-γ-actin antibodies. (B) Quantitative real-time RT-PCR of GFP and GAPDH genes. The ratios of the GFP to GAPDH signals were plotted. No signal was observed in the no-RT control. (C) DNAs prepared from the control and CDK7 siRNA knockdowns were subjected to bisulfite mapping of the CMV promoter and the *GFP* transcribed region. Filled circles, methylated CG dinucleotides; open circles, demethylated CG dinucleotides. (D) Histogram representing quantification of the average methylation (number of methylated CGs/total number of CGs) of the negative control and CDK7 siRNA-treated samples for the CMV or GFP promoter after 48 h of TSA treatment. Each bar represents the average CG methylation of 20 clones.

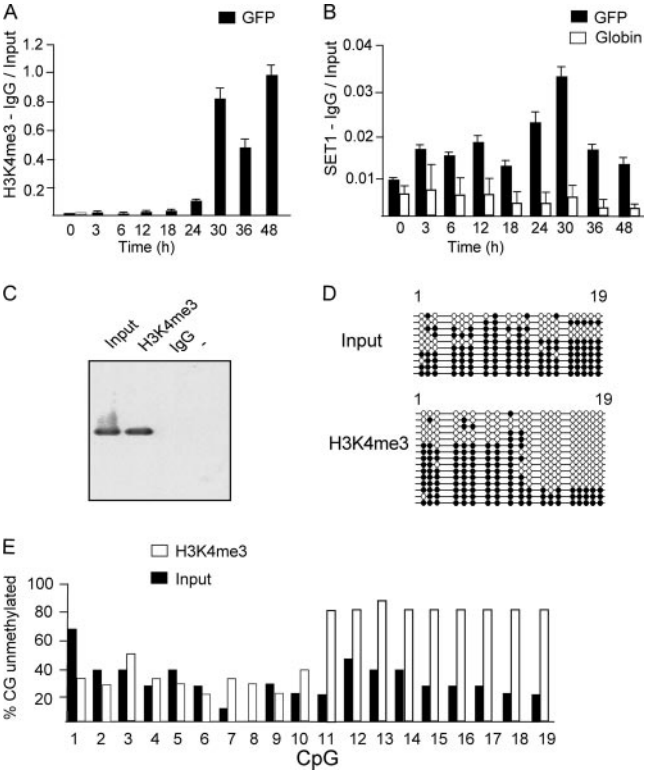

FIG. 6. Time course of association of H3K4me3 with the 5′ end of *GFP* and the DNA methylation status of the associated CMV promoter. In vitro-methylated pCMV-GFP plasmid was transfected into HEK 293 cells, which were treated with TSA at 24 h posttransfection. Cells were harvested at different time intervals post-TSA treatment. (A and B) Cells were subjected to ChIP assay using anti-H3K4me3 (A) or anti-hSET1 (B) antibody or were processed with IgG. The GFP sequence was amplified from purified DNA by quantitative PCR. As a negative control, a region 5 kb upstream of the globin delta gene was amplified by quantitative PCR. No amplification of the globin delta gene was observed in the H3K4me3 samples. (C) Representative bisulfite PCR amplification from input DNA and DNAs purified from immunoprecipitated H3K4me and IgG samples 30 h after TSA addition. (D) The DNAs used for panel C were subjected to bisulfite mapping analysis. Each line represents one clone. Filled circles, methylated CG dinucleotide within the CMV promoter; open circles, demethylated CG dinucleotides. (E) Histogram representing quantification of the methylation status of the input and H3K4me3-bound DNAs at each CG site in the CMV promoter. Each bar represents the average for 10 different clones at each site.

5-aza-cytidine (5-aza-CdR), further confirming their regulation by DNA methylation. A representative of the CT antigens induced by TSA is the G antigen (GAGE) (Table 1). *GAGE* is silent in virtually all adult tissues, with the exception of spermatogonia, placental cells, and some tumors (34). Since the demethylating agent 5-aza-CdR is able to induce this gene (14, 34), it appeared to be a good candidate for further study. RT-PCR of *GAGE* showed that it is induced in response to TSA (Fig. 8B, top panel) as well as 5-aza-CdR (data not shown). Bisulfite mapping analysis of the *GAGE* promoter (Fig. 8A) confirmed that it is highly methylated in HEK 293 cells and becomes demethylated following TSA treatment, with a time course resembling the demethylation of CMV-GFP (compare Fig. 1A and 8A).

DNA demethylation of the endogenous gene *GAGE* is dependent on transcription. We then determined whether demethylation of the transcribed region of *GAGE* is also dependent on transcription. As shown in Fig. 8C, top panel, the first exon of *GAGE* is almost completely methylated in HEK 293 cells, and it became demethylated following TSA treatment (Fig. 8C, middle panel). Inhibition of RNAP II elongation with actinomycin D reduced the extent of DNA demethylation (Fig. 8C, bottom panel). A one-way analysis of variance revealed a

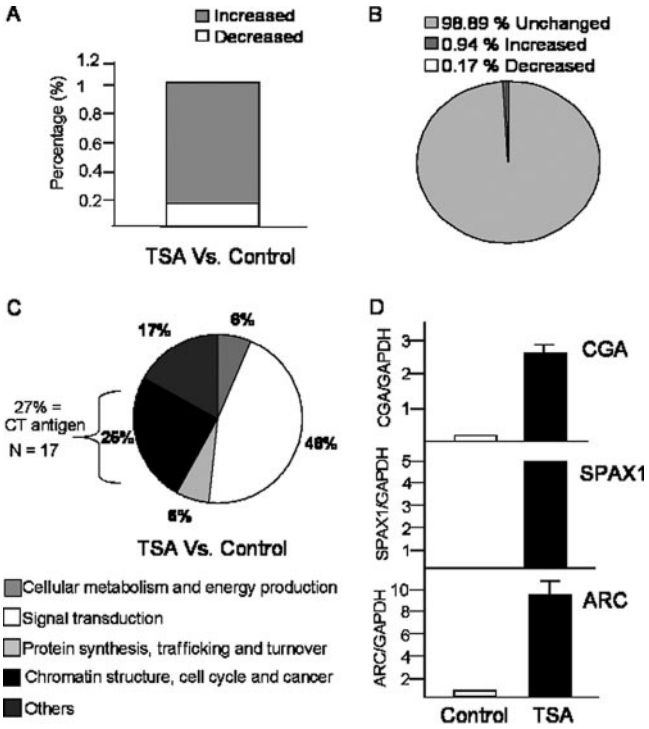

FIG. 7. Gene expression changes following 72 h of treatment of HEK 293 cells with TSA. (A) Percentages of mRNA transcripts increased and decreased by TSA. (B) Pie chart presentation of the percentages of mRNA transcripts increased, decreased, or unchanged by TSA. (C) Distribution of TSA-induced genes over different functional classes. (D) Quantitative real-time PCR validation of the gene array data. Quantitative real-time RT-PCR of the CGA, SPANAX1 (SPAX1), ARC, and GAPDH genes was performed as indicated in Materials and Methods.

highly significant effect of treatment ($F = 24.97$; $P < 0.0001$). Post hoc analysis showed that TSA treatment significantly ($P < 0.001$ for TSA versus controls and TSA versus TSA-plus-actinomycin D treatment) decreased levels of cytosine methylation of CpG sites at the 5′ end of the *GAGE* exon 1 sequence (i.e., increased DNA demethylation). The effect of TSA treatment was blocked ($P > 0.05$ for control versus TSA-plus-actinomycin D treatment) by concomitant treatment of the gene transcription inhibitor actinomycin D (Fig. 8D). These findings are consistent with the idea that transcription is required for DNA demethylation.

To examine the temporal relationship between chromatin modifications and DNA demethylation, we performed ChIP analysis. As shown in Fig. 8B, middle panel, histone H3 acetylation at the *GAGE* promoter started shortly after TSA treatment. DNA demethylation followed histone H3 acetylation, as it does with CMV-GFP (Fig. 1A). Following DNA demethylation, H3K4me3 was associated with the 5′ first exon in both the endogenous gene (Fig. 8B, bottom panel) and the CMV-GFP reporter (Fig. 6A). Interestingly, however, the H3K4me3 association with the first exon of *GAGE* was transient and was reversed between 30 and 48 h after treatment. We do not have, as of yet, an explanation for this difference between *GAGE* and our pCMV-GFP construct. However, when we analyzed the occupancy of SET1 on *GAGE*'s first exon, we found no binding of SET1 (data not shown). Several H3K4 methylases present in mammalian cells, such as MLL, ALL-1, SET9/7, and ALR1-2 (reviewed in reference 33), could be responsible for the H3K4me3 recruitment at the *GAGE* promoter. In addition, it is possible that the discrepancy in H3K4me3 recruitment between the two genes analyzed, *GFP* and *GAGE*, is due to different kinetics of the different enzymes responsible for H3K4me3.

DISCUSSION

Although a hallmark of vertebrate genomes is the correlation between histone acetylation and DNA hypomethylation, the nature of this correlation is still unclear (45). It was demonstrated that DNA methylation silences gene expression and that demethylation activates genes. Therefore, it was expected that demethylation should precede the initiation of transcription and gene expression. However, in this study, we found that transcription is required for active DNA demethylation.

Histone acetylation can be induced either by targeting the gene with a transcription factor that recruits histone acetyltransferases (HATs) or by a pharmacological agent such as TSA. Several studies from our lab as well as others have shown that altering the chromatin by the addition of HDAC inhibitors results in a decrease in DNA methylation in both mammalian cells (15, 62) and *Neurospora* (52). Our replication-independent active DNA demethylation assay demonstrated, as expected, that histone acetylation preceded DNA demethylation (Fig. 1A and B). Moderate levels of histone acetylation (Fig. 1B) were associated with methylated DNA (Fig. 1D); higher levels of histone acetylation were starting to be associated with unmethylated DNA 18 to 24 h after TSA treatment (Fig. 1B and D). These results imply that higher levels of histone acetylation could trigger events needed for DNA demethylation. It is well established that pharmacological DNA demethylation activates gene expression (26), implying a causal relationship between demethylation and gene activation. Unmethylated DNA would enable the interaction of certain transcription factors prohibited from binding by DNA methylation (10). If this model were true, then binding of the transcription machinery to the CMV promoter would follow demethylation, and CMV promoters associated with RNAP II would be unmethylated at the earliest binding time point. However, we found that CMV promoters associated with RNAP II were methylated early after the beginning of their association with RNAP II (18 h) (Fig. 2E). By 24 h, RNAP II was associated with highly unmethylated promoters (Fig. 2E). This suggests that the interaction of a methylated CMV-GFP with RNAP II facilitates demethylation through unknown intermediate steps and raises the provoking hypothesis that early transcription might be the initial cause of DNA demethylation.

We confirmed this hypothesis by using two pharmacological agents, actinomycin D and α-amanitin, which inhibit transcription elongation through different mechanisms (Fig. 4). We further tested this hypothesis by using siRNA knockdown of CDK7, a protein kinase that phosphorylates the RNAP II CTD at serine 5 (17, 56), mediating the transition between transcription initiation and elongation (Fig. 5). The fact that inhibition of transcription elongation by three different mechanisms leads to inhibition of demethylation supports the conclusion that the

TABLE 1. Genes induced by TSA in HEK 293 cells[a]

Accession no.	Fold increase	Array value		Name	Abbreviation
		Control	TSA		
NM_000735.2	317	15	4,798	Glycoprotein hormones alpha polypeptide	CGA
NM_013453.1	114	22	2,508	Sperm protein associated with nucleus X	SPANAX1
M25915.1	85	9	768	Clusterin (complement lysis inhibitor SP-4040-sulfated glycoprotein 2)	CLU
BC004490.1	72	11	790	v-Fos FBJ murine osteosarcoma viral oncogene homolog	FOS
AF193421.1	60	18	1,079	Activity-regulated cytoskeleton-associated protein	ARC
NM_002305.2	53	52	2,778	Lectin galactoside-binding soluble protein 1 (galectin 1)	LGALS1
NM_006183.2	32	59	1,902	Neurotensin	NTS
NM_005794.1	29	124	3,651	Dehydrogenase/reductase (SDR family) member 2	DHRS2
NM_015675.1	29	224	6,412	Growth arrest and DNA-damage-inducible protein beta	GADD45B
BE271470	22	17	367	H2B histone family member A	H2BFA
NM_022661.1	21	104	2,157	SPANX family member C	SPANXC
NM_031272.1	18	15	266	Testis-expressed sequence 14	TEX14
NM_001477.1	18	42	766	G antigen 7B	GAGE7B
AA451996	16	1.287	20,934	H2A histone family member O	H2AFO
NM_005345.3	15	40	604	70-kDa heat shock protein 1A	HSPA1A
N36408	14	16	225	FOS-like antigen 2	FOSL2
NM_021123.1	14	49	666	G antigen 5	GAGE5
NM_014330.2	14	90	1,263	Protein phosphatase 1 regulatory (inhibitor) subunit 15A	PPP1R15A
BC001003.2	13	31	401	Synovial sarcoma X breakpoint 1	SSX1
NM_001473.1	13	56	729	G antigen 3	GAGE3
NM_001472.1	13	41	517	G antigen 2	GAGE2
NM_001476.1	11	97	1,051	G antigen 6	GAGE6
AL021977	11	42	457	v-Maf musculoaponeurotic fibrosarcoma oncogene homolog F (avian)	MAFF
NM_005985.1	11	42	478	Snail homolog 1 (*Drosophila*)	SNAI1
AF133207.1	9	77	664	Protein kinase H11	H11
NM_002426.1	9	58	521	Matrix metalloproteinase 12 (macrophage elastase)	MMP12
NM_000700.1	9	90	781	Annexin A1	ANXA1
NM_001674.1	8	679	5,367	Activating transcription factor 3	ATF3
NM_014178.1	7	67	465	Syntaxin binding protein 6 (amisyn)	STXBP6

[a] HEK 293 cells were either treated with TSA (300 nM) for 72 h in duplicate or left untreated as a control. Total RNA was subjected to a differential expression microarray analysis using HuGeneFL DNA microarrays containing oligonucleotides specific for approximately 25,000 human transcripts, as described in Materials and Methods. The table lists representative genes which showed consistent changes in both experiments.

effects observed were not results of idiosyncrasies of these agents but rather of their common activity, i.e., inhibition of transcription. To exclude the possibility that inhibition of transcription could act indirectly by changing the mRNA level of a high-turnover factor required for DNA demethylation, we treated the cells with cycloheximide. Cycloheximide blocked protein synthesis and should have blocked the expression of any high-turnover factor. However, cycloheximide did not inhibit DNA demethylation (Fig. 4).

The idea that transcription, rather than just RNAP II binding per se, is required for demethylation is supported by the difference observed in the kinetics of demethylation of the transcribed regions of the GFP gene and the CMV promoter. If binding of RNAP II were the rate-limiting step for demethylation, we would expect the promoter, which was the landing pad of RNAP II, to be demethylated first. However, our data suggest that demethylation at the promoter lags behind demethylation of the transcribed region of the reporter gene (Fig. 3). These data are consistent with the hypothesis that the progression of transcription recruits demethylases to the gene and that this demethylation eventually spreads to the promoter region. In addition, the fact that DNA demethylation does not proceed beyond the position where transcription is terminated supports the hypothesis that demethylation is linked to the passage of the transcription machinery (Fig. 4G).

Interestingly, we found that DNA demethylation at the promoter is followed by H3K4me3 of histones associated with the transcribed region of GFP (Fig. 6). H3K4me3 at the coding region of genes has been postulated to function as a memory of active transcription in yeast (38) as well as higher organisms (50). Using a combination of ChIP and bisulfite mapping, we showed that the DNA associated with H3K4me3 was hypomethylated compared with the unbound population of CMV promoters (Fig. 6). This is consistent with the hypothesis that H3K4me3 tags on demethylation of DNA. In agreement, the loss of Lsh, a modulator of CG DNA methylation, results in increased H3K4me3, and treatment with the DNA methylation inhibitor 5-aza-CdR also results in increased H3K4me3 (65).

If RNAP II can bind and transcribe methylated DNA, what is the purpose of DNA demethylation? The idea that RNAP II progression along a gene might affect epigenetic programming of gene expression has been suggested before and is supported by other evidence. For example, RNAP II interacts with chromatin remodeling enzymes, such as BRG1, a member of the SWI/SNF chromatin remodeling complex; with HATs, such as CBP (8, 37); and with chromatin-modifying enzymes, such as SET1 (38). MLL1, a human equivalent of yeast SET1, associates with highly expressed transcripts (22). The passage of RNAP II transcribing a gene was proposed to be coupled to mechanisms that propagate the breakdown and reprogram-

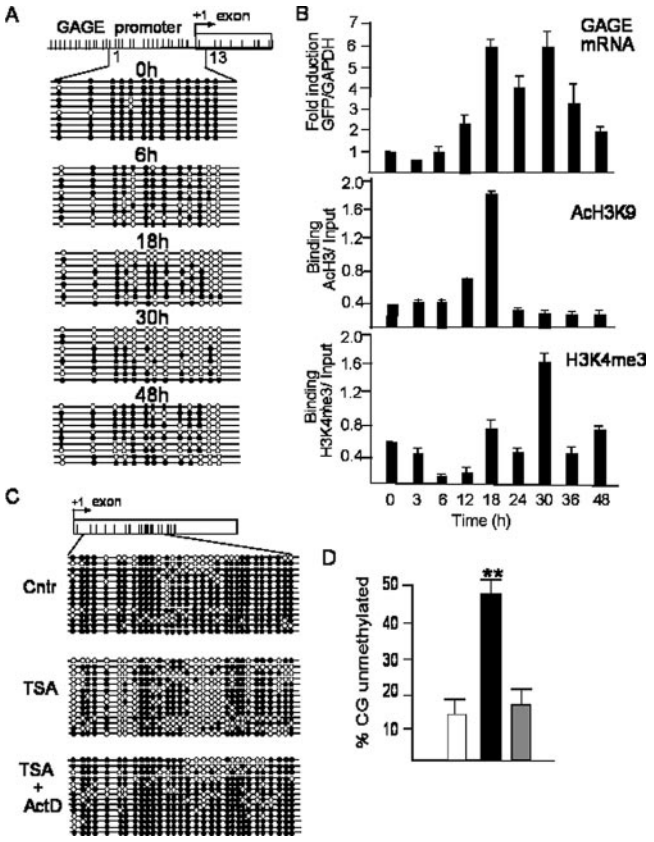

FIG. 8. The *GAGE* promoter is demethylated in response to TSA treatment. HEK 293 cells were treated with TSA and harvested after different times of TSA treatment. (A) Physical map of the *GAGE* promoter region analyzed by bisulfite mapping. (B) (Top) Kinetics of *GAGE* expression after TSA treatment. Quantitative real-time RT-PCR of the GAGE and GAPDH genes was performed. The *x*-fold induction of the GAGE to GAPDH signals was plotted. (Middle) ChIP assay using anti-H3K9Ac antibody. Results of quantitative real-time PCR of the *GAGE* promoter are shown. (Bottom) ChIP assay using anti-H3K4me3 antibody. Results of quantitative real-time PCR of the *GAGE* exon are shown. (C) HEK 293 cells were treated with TSA for 30 h or left untreated as a control. After 18 h of treatment, cells were either treated or not treated (control) with a final concentration of 1 μg/ml actinomycin D (ActD) for 12 h. DNAs were subjected to bisulfite mapping analysis. Filled circles, methylated CG dinucleotides within the CMV promoter; open circles, demethylated CG dinucleotides. (D) Percentages of unmethylated CGs were calculated by measuring the percent demethylation per clone per treatment for the experiments shown in panel C. Tukey's multiple comparison test was used to calculate the statistical significance.

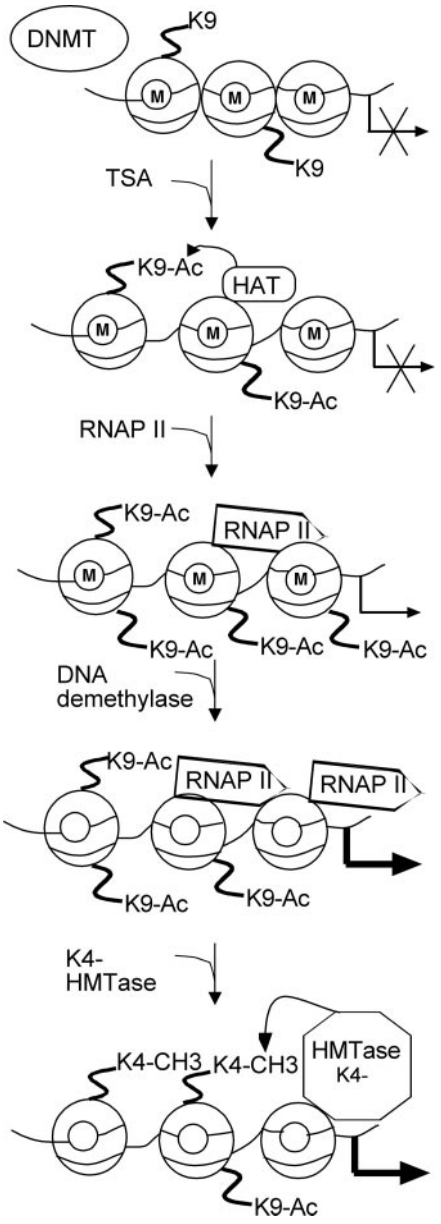

FIG. 9. RNAP II transcription is required for DNA demethylation. Pharmacological induction of a gene with TSA triggers limited histone acetylation by the enzymatic activity of HATs. Following limited histone acetylation, RNAP II binds the methylated promoters. Progression of RNAP II along the gene facilitates DNA demethylation, which results in robust acetylation and transcription and in recruitment of histone methylases to methylate lysine 4 at the coding region of the gene. DNMT, DNA methyltransferases.

ming of chromatin (40). Thus, it was proposed that RNAP II transmits the change in promoter accessibility caused by transcription factor binding, recruitment of HAT, and histone acetylation down the gene, thus translating early changes in promoter activity to more stable changes in chromatin structure (40).

Figure 9 illustrates our current model for the mechanism of active DNA demethylation in response to a signal triggering histone acetylation. Histone acetylation enables initial recruitment of RNAP II to the methylated promoter. The early progression of RNAP II along the gene at the time of transcription either facilitates or directly recruits DNA demethylases, which demethylate the transcribed region, followed by demethylation of the promoter. Demethylation is a prerequisite for robust gene expression. The demethylated promoter significantly increased its association with RNAP II and augmented the acetylation of histone tails, resulting in elevated levels of GFP expression and stable epigenetic programming of the gene, as indicated by the H3K4me3 tails. It is also tempting to speculate that transcription of a gene is required for maintaining an unmethylated and epigenetically programmed gene. It is pos-

sible, therefore, that cessation of transcription might lead to remethylation of the gene, which might explain many observations showing remethylation of genes which were previously silenced in culture (58). Thus, transcription and epigenetic programming by demethylation might act coordinately in a positive feedback loop to maintain an active gene.

We have shown here the existence of transcription-dependent active DNA demethylation, but it remains to be seen whether all DNA demethylation-methylation events are similarly controlled. The demethylation seen in the CMV promoter and the downstream transcribed *GFP* sequences creates an unmethylated CG-rich area which resembles CG-rich promoters and the first exon regions of several housekeeping genes. We show here, however, that TSA-triggered DNA demethylation and H3K4me3 are not limited to ectopically methylated viral promoters but also target the promoter and first exon of the CT antigen gene *GAGE* (Fig. 8). This gene is methylated in all somatic tissues but is hypomethylated in the testis and in cancer. The demethylation of this gene, like the demethylation of the CMV-driven reporter gene, is transcription dependent since it is inhibited by actinomycin D. This class of genes was found in a recent comprehensive analysis of human promoters to be regulated dynamically by DNA methylation (63). It stands to reason that RNA transcription is specifically involved in demethylation of this group of genes. However, it is unclear whether this mechanism applies to other genes, notably sparsely methylated and CG-poor genes or CG-rich islands containing promoters.

A recent comprehensive analysis of the human "methylome" revealed that promoters with sparsely distributed CGs are methylated irrespective of their state of expression. Another interesting group are the CG-rich islands, which are unmethylated irrespective of their state of expression, suggesting that transcription cannot be involved in demethylation and maintenance of hypomethylation of this group of promoters. Interestingly, CG-rich islands are associated with a specific chromatin modification, H3K4 dimethylation, which usually marks active chromatin regions. It is proposed that this histone modification might be involved in demethylation of CG-rich islands (63). Future experiments are required to determine how H3K4 dimethylation specifies an unmethylated sequence, whether it stimulates active demethylation, or whether it protects from de novo methylation.

Interestingly, a recent paper analyzing genomic methylation in *Arabidopsis thaliana* showed that DNA methylation is biased away from gene ends, suggesting a dependence on RNA polymerase transit (69). Moreover, the authors grouped the genes according to their expression levels and showed that genic methylation is strongly influenced by transcription: moderately transcribed genes are more likely to be methylated, whereas highly and weakly transcribed genes are less likely to be methylated. In addition, this study showed that short methylated genes are poorly expressed and that a loss of methylation leads to enhanced gene expression. The CMV-GFP reporter tested here seems to follow a similar course, since it was demethylated once the state of transcription was changed from basal levels to high transcription upon the addition of TSA.

There are convincing examples of active, replication-independent DNA demethylation during development. Genes that are highly methylated in the paternal genome are rapidly demethylated in the zygote only hours after fertilization, before the first round of DNA replication commences (42). Examples of gene-specific active DNA demethylation in differentiating cells include the immunoglobulin gene locus during B-cell maturation (16, 30), the muscle-specific alpha-actin gene (44), and the vitellogenin genes in chicken tissues upon estrogen stimulation (64). Active demethylation was reported for the myosin gene in differentiating myoblast cells (35), for the interleukin-2 gene upon T-cell activation (4), and for the gamma interferon gene upon antigen exposure of memory CD8 T cells (28). For these examples, transcription factor interaction was suggested to be critical for DNA demethylation; however, a detailed time course analysis of the chromatin events leading to active DNA demethylation was missing in these studies. We might need to revisit these examples of active demethylation to define the requirements for transcription.

A recently published paper from our lab (43) shows that TSA induces both global acetylation and global DNA demethylation. However, certain sequences, such as repetitive Alu sequences, showed no change in DNA methylation upon TSA treatment, suggesting that even though there are global changes in DNA methylation, they reflect changes in specific promoters, not the entire genome, which would have happened if demethylation were totally passive. This important observation suggests that TSA induces DNA demethylation by an active mechanism. Moreover, this study also showed that inhibition of DNA replication by hydroxyurea did not inhibit TSA-induced DNA demethylation under conditions where there was no cell division and no DNA synthesis. In agreement with our suggestion here, it was shown that TSA as well as valproate can induce DNA demethylation in nondividing tissue such as the brain (15, 62). However, unlike the case with the nonreplicating reporter plasmid, where demethylation must be active, it is hard to formally exclude the possibility that a passive process demethylates endogenous genes. Nevertheless, we show a good correspondence between reporter gene demethylation and that of the endogenous gene which is consistent with the hypothesis that similar processes are involved in both cases.

What is the mechanism that drives DNA demethylation upon transcription elongation? Two alternative mechanisms can explain this observation. Firstly, transcription has been shown to set a platform for histone eviction (51), and this event allows a more open configuration of the chromatin which, in turn, may favor demethylase access to the DNA. Alternatively, it is possible that RNAP II interacts with the DNA demethylase. Future experiments are required to identify the demethylase involved in this process and to determine whether it interacts with RNAP II.

The mechanism of active DNA demethylation is challenging because it requires the disruption of a carbon-carbon bond between the methyl group at position 5 and the cytosine ring. One potential mechanism avoiding this difficult chemical reaction is through the action of 5-methylcytosine DNA glycosylases (27). These enzymes remove the 5-methylcytosine, and then local DNA repair removes the abasic nucleotide and introduces an unmethylated cytidylate (60). G/T-mismatch-repair DNA glycosylases, such as the methyl CpG binding protein MBD4, were found to have DNA glycosylase activity (67, 68). Genetic evidence in *Arabidopsis* supports these findings, since mutations in the

DNA glycosylase ROS1 cause DNA hypermethylation and transcriptional gene silencing (20). A recent report shows that ROS1 has 5-methylcytosine DNA glycosylase activity against several DNA substrates in vitro (1). However, transcription-dependent DNA demethylation through this mechanism might create a serious threat to the genome's integrity.

Our laboratory has proposed a second mechanism of DNA demethylation through direct removal of the methyl moiety from the DNA. The methyl CpG binding protein MBD2 was reported to belong to a new class of enzymes that can directly demethylate DNA (3). There was significant controversy regarding the identification of MBD2 as a demethylase because of reported irreproducibility of the demethylation activity in vitro (39). Future experiments are required to understand whether MBD2 or other DNA demethylases are responsible for the transcription-dependent demethylation described here. These experiments are currently in progress.

Although the data presented here pose many new questions, they also present a new and unexpected paradigm of gene activation whereby transcription by RNAP II plays a causal role in epigenetic programming by DNA demethylation. These data provide an explanation for the long-established correlation of gene activity and DNA hypomethylation.

ACKNOWLEDGMENTS

This study was supported by a grant from the National Cancer Institute of Canada to M.S. A.C.D. was supported by a CIHR training grant.

We thank Luciana Molinero for advice and Marianne Godbout, Isabelle Guillet, and Andre Ponton from Genome Quebec for technical assistance with the real-time PCR quantifications.

REFERENCES

1. **Agius, F., A. Kapoor, and J. K. Zhu.** 2006. Role of the Arabidopsis DNA glycosylase/lyase ROS1 in active DNA demethylation. Proc. Natl. Acad. Sci. USA **103:**11796–11801.
2. **Baylin, S. B., M. Esteller, M. R. Rountree, K. E. Bachman, K. Schuebel, and J. G. Herman.** 2001. Aberrant patterns of DNA methylation, chromatin formation and gene expression in cancer. Hum. Mol. Genet. **10:**687–692.
3. **Bhattacharya, S. K., S. Ramchandani, N. Cervoni, and M. Szyf.** 1999. A mammalian protein with specific demethylase activity for mCpG DNA. Nature **397:**579–583.
4. **Bruniquel, D., and R. H. Schwartz.** 2003. Selective, stable demethylation of the interleukin-2 gene enhances transcription by an active process. Nat. Immunol. **4:**235–240.
5. **Bushnell, D. A., K. D. Westover, R. E. Davis, and R. D. Kornberg.** 2004. Structural basis of transcription: an RNA polymerase II-TFIIB cocrystal at 4.5 angstroms. Science **303:**983–988.
6. **Cervoni, N., N. Detich, S. B. Seo, D. Chakravarti, and M. Szyf.** 2002. The oncoprotein Set/TAF-1beta, an inhibitor of histone acetyltransferase, inhibits active demethylation of DNA, integrating DNA methylation and transcriptional silencing. J. Biol. Chem. **277:**25026–25031.
7. **Cervoni, N., and M. Szyf.** 2001. Demethylase activity is directed by histone acetylation. J. Biol. Chem. **276:**40778–40787.
8. **Cho, H., G. Orphanides, X. Sun, X. J. Yang, V. Ogryzko, E. Lees, Y. Nakatani, and D. Reinberg.** 1998. A human RNA polymerase II complex containing factors that modify chromatin structure. Mol. Cell. Biol. **18:**5355–5363.
9. **Clark, S. J., J. Harrison, C. L. Paul, and M. Frommer.** 1994. High sensitivity mapping of methylated cytosines. Nucleic Acids Res. **22:**2990–2997.
10. **Comb, M., and H. M. Goodman.** 1990. CpG methylation inhibits proenkephalin gene expression and binding of the transcription factor AP-2. Nucleic Acids Res. **18:**3975–3982.
11. **Conaway, J. W., A. Shilatifard, A. Dvir, and R. C. Conaway.** 2000. Control of elongation by RNA polymerase II. Trends Biochem. Sci. **25:**375–380.
12. **Crane-Robinson, C., F. A. Myers, T. R. Hebbes, A. L. Clayton, and A. W. Thorne.** 1999. Chromatin immunoprecipitation assays in acetylation mapping of higher eukaryotes. Methods Enzymol. **304:**533–547.
13. **D'Alessio, A. C., and M. Szyf.** 2006. Epigenetic tete-a-tete: the bilateral relationship between chromatin modifications and DNA methylation. Biochem. Cell Biol. **84:**463–476.
14. **De Backer, O., K. C. Arden, M. Boretti, V. Vantomme, C. De Smet, S. Czekay, C. S. Viars, E. De Plaen, F. Brasseur, P. Chomez, B. Van den Eynde, T. Boon, and P. van der Bruggen.** 1999. Characterization of the GAGE genes that are expressed in various human cancers and in normal testis. Cancer Res. **59:**3157–3165.
15. **Dong, E., A. Guidotti, D. R. Grayson, and E. Costa.** 2007. Histone hyperacetylation induces demethylation of reelin and 67-kDa glutamic acid decarboxylase promoters. Proc. Natl. Acad. Sci. USA **104:**4676–4681.
16. **Frank, D., M. Lichtenstein, Z. Paroush, Y. Bergman, M. Shani, A. Razin, and H. Cedar.** 1990. Demethylation of genes in animal cells. Philos. Trans. R. Soc. Lond. B **326:**241–251.
17. **Gebara, M. M., C. Drevon, S. A. Harcourt, H. Steingrimsdottir, M. R. James, J. F. Burke, C. F. Arlett, and A. R. Lehmann.** 1987. Inactivation of a transfected gene in human fibroblasts can occur by deletion, amplification, phenotypic switching, or methylation. Mol. Cell. Biol. **7:**1459–1464.
18. **Golub, T. R., D. K. Slonim, P. Tamayo, C. Huard, M. Gaasenbeek, J. P. Mesirov, H. Coller, M. L. Loh, J. R. Downing, M. A. Caligiuri, C. D. Bloomfield, and E. S. Lander.** 1999. Molecular classification of cancer: class discovery and class prediction by gene expression monitoring. Science **286:**531–537.
19. **Gong, X. Q., Y. A. Nedialkov, and Z. F. Burton.** 2004. Alpha-amanitin blocks translocation by human RNA polymerase II. J. Biol. Chem. **279:**27422–27427.
20. **Gong, Z., T. Morales-Ruiz, R. R. Ariza, T. Roldan-Arjona, L. David, and J. K. Zhu.** 2002. ROS1, a repressor of transcriptional gene silencing in Arabidopsis, encodes a DNA glycosylase/lyase. Cell **111:**803–814.
21. **Guccione, E., F. Martinato, G. Finocchiaro, L. Luzi, L. Tizzoni, V. Dall'Olio, G. Zardo, C. Nervi, L. Bernard, and B. Amati.** 2006. Myc-binding-site recognition in the human genome is determined by chromatin context. Nat. Cell Biol. **8:**764–770.
22. **Guenther, M. G., R. G. Jenner, B. Chevalier, T. Nakamura, C. M. Croce, E. Canaani, and R. A. Young.** 2005. Global and Hox-specific roles for the MLL1 methyltransferase. Proc. Natl. Acad. Sci. USA **102:**8603–8608.
23. **Hayashi, H., G. Nagae, S. Tsutsumi, K. Kaneshiro, T. Kozaki, A. Kaneda, H. Sugisaki, and H. Aburatani.** 2007. High-resolution mapping of DNA methylation in human genome using oligonucleotide tiling array. Hum. Genet. **120:**701–711.
24. **Jackson, J. P., A. M. Lindroth, X. Cao, and S. E. Jacobsen.** 2002. Control of CpNpG DNA methylation by the KRYPTONITE histone H3 methyltransferase. Nature **416:**556–560.
25. **Johnson, L., X. Cao, and S. Jacobsen.** 2002. Interplay between two epigenetic marks. DNA methylation and histone H3 lysine 9 methylation. Curr. Biol. **12:**1360–1367.
26. **Jones, P. A.** 1985. Effects of 5-azacytidine and its 2′-deoxyderivative on cell differentiation and DNA methylation. Pharmacol. Ther. **28:**17–27.
27. **Jost, J. P., S. Schwarz, D. Hess, H. Angliker, F. V. Fuller-Pace, H. Stahl, S. Thiry, and M. Siegmann.** 1999. A chicken embryo protein related to the mammalian DEAD box protein p68 is tightly associated with the highly purified protein-RNA complex of 5-MeC-DNA glycosylase. Nucleic Acids Res. **27:**3245–3252.
28. **Kersh, E. N., D. R. Fitzpatrick, K. Murali-Krishna, J. Shires, S. H. Speck, J. M. Boss, and R. Ahmed.** 2006. Rapid demethylation of the IFN-γ gene occurs in memory but not naive CD8 T cells. J. Immunol. **176:**4083–4093.
29. **Kimura, H., K. Sugaya, and P. R. Cook.** 2002. The transcription cycle of RNA polymerase II in living cells. J. Cell Biol. **159:**777–782.
30. **Kirillov, A., B. Kistler, R. Mostoslavsky, H. Cedar, T. Wirth, and Y. Bergman.** 1996. A role for nuclear NF-kappaB in B-cell-specific demethylation of the Igkappa locus. Nat. Genet. **13:**435–441.
31. **Komarnitsky, P., E. J. Cho, and S. Buratowski.** 2000. Different phosphorylated forms of RNA polymerase II and associated mRNA processing factors during transcription. Genes Dev. **14:**2452–2460.
32. **Lemon, B., and R. Tjian.** 2000. Orchestrated response: a symphony of transcription factors for gene control. Genes Dev. **14:**2551–2569.
33. **Li, B., M. Carey, and J. L. Workman.** 2007. The role of chromatin during transcription. Cell **128:**707–719.
34. **Li, J., Y. Yang, T. Fujie, K. Baba, H. Ueo, M. Mori, and T. Akiyoshi.** 1996. Expression of BAGE, GAGE, and MAGE genes in human gastric carcinoma. Clin. Cancer Res. **2:**1619–1625.
35. **Lucarelli, M., A. Fuso, R. Strom, and S. Scarpa.** 2001. The dynamics of myogenin site-specific demethylation is strongly correlated with its expression and with muscle differentiation. J. Biol. Chem. **276:**7500–7506.
36. **Naar, A. M., B. D. Lemon, and R. Tjian.** 2001. Transcriptional coactivator complexes. Annu. Rev. Biochem. **70:**475–501.
37. **Neish, A. S., S. F. Anderson, B. P. Schlegel, W. Wei, and J. D. Parvin.** 1998. Factors associated with the mammalian RNA polymerase II holoenzyme. Nucleic Acids Res. **26:**847–853.
38. **Ng, H. H., F. Robert, R. A. Young, and K. Struhl.** 2003. Targeted recruitment of Set1 histone methylase by elongating Pol II provides a localized mark and memory of recent transcriptional activity. Mol. Cell **11:**709–719.
39. **Ng, H. H., Y. Zhang, B. Hendrich, C. A. Johnson, B. M. Turner, H. Erdjument-Bromage, P. Tempst, D. Reinberg, and A. Bird.** 1999. MBD2 is a transcriptional repressor belonging to the MeCP1 histone deacetylase complex. Nat. Genet. **23:**58–61.

40. **Orphanides, G., and D. Reinberg.** 2000. RNA polymerase II elongation through chromatin. Nature **407:**471–475.
41. **Orphanides, G., and D. Reinberg.** 2002. A unified theory of gene expression. Cell **108:**439–451.
42. **Oswald, J., S. Engemann, N. Lane, W. Mayer, A. Olek, R. Fundele, W. Dean, W. Reik, and J. Walter.** 2000. Active demethylation of the paternal genome in the mouse zygote. Curr. Biol. **10:**475–478.
43. **Ou, J. N., J. Torrisani, A. Unterberger, N. Provencal, K. Shikimi, M. Karimi, T. J. Ekstrom, and M. Szyf.** 2007. Histone deacetylase inhibitor trichostatin A induces global and gene-specific DNA demethylation in human cancer cell lines. Biochem. Pharmacol. **73:**1297–1307.
44. **Paroush, Z., I. Keshet, J. Yisraeli, and H. Cedar.** 1990. Dynamics of demethylation and activation of the alpha-actin gene in myoblasts. Cell **63:**1229–1237.
45. **Razin, A.** 1998. CpG methylation, chromatin structure and gene silencing—a three-way connection. EMBO J. **17:**4905–4908.
46. **Razin, A., and H. Cedar.** 1977. Distribution of 5-methylcytosine in chromatin. Proc. Natl. Acad. Sci. USA **74:**2725–2728.
47. **Razin, A., and H. Cedar.** 1984. DNA methylation in eukaryotic cells. Int. Rev. Cytol. **92:**159–185.
48. **Razin, A., A. Levine, T. Kafri, S. Agostini, T. Gomi, and G. L. Cantoni.** 1988. Relationship between transient DNA hypomethylation and erythroid differentiation of murine erythroleukemia cells. Proc. Natl. Acad. Sci. USA **85:** 9003–9006.
49. **Santos-Rosa, H., R. Schneider, A. J. Bannister, J. Sherriff, B. E. Bernstein, N. C. Emre, S. L. Schreiber, J. Mellor, and T. Kouzarides.** 2002. Active genes are tri-methylated at K4 of histone H3. Nature **419:**407–411.
50. **Schneider, R., A. J. Bannister, F. A. Myers, A. W. Thorne, C. Crane-Robinson, and T. Kouzarides.** 2004. Histone H3 lysine 4 methylation patterns in higher eukaryotic genes. Nat. Cell Biol. **6:**73–77.
51. **Schwabish, M. A., and K. Struhl.** 2004. Evidence for eviction and rapid deposition of histones upon transcriptional elongation by RNA polymerase II. Mol. Cell. Biol. **24:**10111–10117.
52. **Selker, E. U.** 1998. Trichostatin A causes selective loss of DNA methylation in Neurospora. Proc. Natl. Acad. Sci. USA **95:**9430–9435.
53. **Serizawa, H., T. P. Makela, J. W. Conaway, R. C. Conaway, R. A. Weinberg, and R. A. Young.** 1995. Association of Cdk-activating kinase subunits with transcription factor TFIIH. Nature **374:**280–282.
54. **Shiekhattar, R., F. Mermelstein, R. P. Fisher, R. Drapkin, B. Dynlacht, H. C. Wessling, D. O. Morgan, and D. Reinberg.** 1995. Cdk-activating kinase complex is a component of human transcription factor TFIIH. Nature **374:** 283–287.
55. **Sigalotti, L., S. Coral, G. Nardi, A. Spessotto, E. Cortini, I. Cattarossi, F. Colizzi, M. Altomonte, and M. Maio.** 2002. Promoter methylation controls the expression of MAGE2, 3 and 4 genes in human cutaneous melanoma. J. Immunother. **25:**16–26.
56. **Spilianakis, C., A. Kretsovali, T. Agalioti, T. Makatounakis, D. Thanos, and J. Papamatheakis.** 2003. CIITA regulates transcription onset via Ser5-phosphorylation of RNA Pol II. EMBO J. **22:**5125–5136.
57. **Strahl, B. D., and C. D. Allis.** 2000. The language of covalent histone modifications. Nature **403:**41–45.
58. **Szyf, M., D. S. Milstone, B. P. Schimmer, K. L. Parker, and J. G. Seidman.** 1990. cis modification of the steroid 21-hydroxylase gene prevents its expression in the Y1 mouse adrenocortical tumor cell line. Mol. Endocrinol. **4:**1144–1152.
59. **Tamaru, H., X. Zhang, D. McMillen, P. B. Singh, J. Nakayama, S. I. Grewal, C. D. Allis, X. Cheng, and E. U. Selker.** 2003. Trimethylated lysine 9 of histone H3 is a mark for DNA methylation in Neurospora crassa. Nat. Genet. **34:**75–79.
60. **Vairapandi, M., and N. J. Duker.** 1993. Enzymic removal of 5-methylcytosine from DNA by a human DNA-glycosylase. Nucleic Acids Res. **21:**5323–5327.
61. **Vire, E., C. Brenner, R. Deplus, L. Blanchon, M. Fraga, C. Didelot, L. Morey, A. Van Eynde, D. Bernard, J. M. Vanderwinden, M. Bollen, M. Esteller, L. Di Croce, Y. de Launoit, and F. Fuks.** 2005. The Polycomb group protein EZH2 directly controls DNA methylation. Nature **439:**871–874.
62. **Weaver, I. C., N. Cervoni, F. A. Champagne, A. C. D'Alessio, S. Sharma, J. R. Seckl, S. Dymov, M. Szyf, and M. J. Meaney.** 2004. Epigenetic programming by maternal behavior. Nat. Neurosci. **7:**847–854.
63. **Weber, M., I. Hellmann, M. B. Stadler, L. Ramos, S. Paabo, M. Rebhan, and D. Schubeler.** 2007. Distribution, silencing potential and evolutionary impact of promoter DNA methylation in the human genome. Nat. Genet. **39:**457–466.
64. **Wilks, A. F., P. J. Cozens, I. W. Mattaj, and J. P. Jost.** 1982. Estrogen induces a demethylation at the 5′ end region of the chicken vitellogenin gene. Proc. Natl. Acad. Sci. USA **79:**4252–4255.
65. **Yan, Q., J. Huang, T. Fan, H. Zhu, and K. Muegge.** 2003. Lsh, a modulator of CpG methylation, is crucial for normal histone methylation. EMBO J. **22:**5154–5162.
66. **Zhang, Y., and D. Reinberg.** 2001. Transcription regulation by histone methylation: interplay between different covalent modifications of the core histone tails. Genes Dev. **15:**2343–2360.
67. **Zhu, B., Y. Zheng, H. Angliker, S. Schwarz, S. Thiry, M. Siegmann, and J. P. Jost.** 2000. 5-Methylcytosine DNA glycosylase activity is also present in the human MBD4 (G/T mismatch glycosylase) and in a related avian sequence. Nucleic Acids Res. **28:**4157–4165.
68. **Zhu, B., Y. Zheng, D. Hess, H. Angliker, S. Schwarz, M. Siegmann, S. Thiry, and J. P. Jost.** 2000. 5-Methylcytosine-DNA glycosylase activity is present in a cloned G/T mismatch DNA glycosylase associated with the chicken embryo DNA demethylation complex. Proc. Natl. Acad. Sci. USA **97:**5135–5139.
69. **Zilberman, D., M. Gehring, R. K. Tran, T. Ballinger, and S. Henikoff.** 2007. Genome-wide analysis of Arabidopsis thaliana DNA methylation uncovers an interdependence between methylation and transcription. Nat. Genet. **39:**61–69.